

The binding of DnaG to DnaB stimulates the activities of DnaB (1) and stabilizes the three-fold conformation of the DnaB NTDs. This suggests that the three-fold symmetric state represents an activated form of DnaB; therefore, it seems doubtful that the DNA translocation mechanism of DnaB involves transitions between six- and three-fold symmetries. Both DnaB and the T7 gp4 proteins require a stable hexamer for NTPase and helicase activity (9, 18). Therefore, the DnaG-mediated stimulation of the activities of DnaB could also result from the increased stability of the hexamer produced by the binding of DnaG, which is consistent with the observation that although the isolated C2 subdomain of the HBD can bind DnaB, both subdomains of the HBD are required for the stimulation of the activities of DnaB (16). Although the presence of DnaG at the replication fork in *E. coli* has been shown to be distributive (31), the binding of only one molecule of DnaG to DnaB would be sufficient to stabilize the three-fold conformation of DnaB. The closed circular structure of the NTD collar could also contribute to the stimulation of the helicase activity by keeping the two ssDNA strands topologically separated during unwinding. In addition the topological linking of DnaB to the DNA also would ensure that the two molecules could not easily disengage, thus increasing the processivity of the reaction. Kinetic analysis has shown that isolated DnaB is only a moderately processive enzyme, and it is assumed that it gains the processivity needed to replicate the genome from other components of the replication fork (32). A similar processivity role has also been suggested for the unrelated NTD of the papillomavirus E1 helicase (20).

The NTD collar may also provide an additional binding site for ssDNA. The interior surface of the NTD collar exhibits three distinct sites of positive electrostatic potential separated by regions of negative electrostatic potential (Fig. 4A). These positive sites are consistent with their binding DNA, contain residues that are conserved across DnaB species, and are well positioned for binding the ssDNA as it emanates from the CTD ring (Fig. 4). Nuclease protection and fluorescence energy transfer studies have also suggested the presence of a second ssDNA binding site at the N terminus of DnaB (33).

It is now possible to construct a model of the complex between DnaB and DnaG that illuminates how they cooperatively work together and stimulate each other's activities. The N terminus of each HBD is situated adjacent to the central channel of DnaB (Fig. 3), thereby positioning the N-terminal ZBD and RPD of full-length DnaG directly above the central channel (Fig. 4B). Thus, the structure of the RPD-ZBD fragment (34) can be positioned relative to the HBD in a manner that orients the primase active site with the proposed N-terminal ssDNA binding site of

DnaB and is consistent with the structure of the truncated T7 gp4 helicase-primase heptamer (21). The structure of the complex between DnaB and HBD, and our modeling of the complex between the full-length proteins, is consistent with the possibility that DnaB stimulates the activity of DnaG by increasing the local concentration of the ssDNA substrate and by ensuring that multiple DnaG subunits are in close proximity to each other (35) (Fig. 4B). The latter is important because the RPD and ZBD function have been shown to function in trans, with each domain provided by a separate subunit (35).

References and Notes

- J. E. Corn, J. M. Berger, *Nucleic Acids Res.* **34**, 4082 (2006).
- J. H. LeBowitz, R. McMacken, *J. Biol. Chem.* **261**, 4738 (1986).
- S. Yang *et al.*, *J. Mol. Biol.* **321**, 839 (2002).
- R. Nunez-Ramirez *et al.*, *J. Mol. Biol.* **357**, 1063 (2006).
- M. J. Jezewska, S. Rajendran, D. Bujalowski, W. Bujalowski, *J. Biol. Chem.* **273**, 10515 (1998).
- D. L. Kaplan, *J. Mol. Biol.* **301**, 285 (2000).
- S. Bailey, W. K. Eliason, T. A. Steitz, *Nucleic Acids Res.* **35**, 4728 (2007).
- N. Nakayama, N. Arai, Y. Kaziro, K. Arai, *J. Biol. Chem.* **259**, 88 (1984).
- L. E. Bird, H. Pan, P. Soutlanas, D. B. Wigley, *Biochemistry* **39**, 171 (2000).
- P. Mesa, J. C. Alonso, S. Ayora, *J. Mol. Biol.* **357**, 1077 (2006).
- K. Tougu, K. J. Marians, *J. Biol. Chem.* **271**, 21391 (1996).
- K. Syson, J. Thirlway, A. M. Hounslow, P. Soutlanas, J. P. Waltho, *Structure* **13**, 609 (2005).
- A. J. Oakley *et al.*, *J. Biol. Chem.* **280**, 11495 (2005).
- Y. B. Lu, S. Bhattacharyya, M. A. Griep, *Proc. Natl. Acad. Sci. U.S.A.* **93**, 12902 (1996).
- A. V. Mitkova, S. M. Khopde, S. B. Biswas, *J. Biol. Chem.* **278**, 52253 (2003).
- J. Thirlway, P. Soutlanas, *J. Bacteriol.* **188**, 1534 (2006).
- Materials and methods are available as supporting material on Science Online.
- M. R. Singleton, M. R. Sawaya, T. Ellenberger, D. B. Wigley, *Cell* **101**, 589 (2000).
- S. B. Biswas, P. H. Chen, E. E. Biswas, *Biochemistry* **33**, 11307 (1994).
- E. J. Enemark, L. Joshua-Tor, *Nature* **422**, 270 (2006).
- W. Bujalowski, M. J. Jezewska, *Biochemistry* **34**, 8513 (1995).
- E. A. Toth, Y. Li, M. R. Sawaya, Y. Cheng, T. Ellenberger, *Mol. Cell* **12**, 1113 (2003).
- M. R. Sawaya, S. Guo, S. Tabor, C. C. Richardson, T. Ellenberger, *Cell* **99**, 167 (1999).
- D. J. Crampton, S. Guo, D. E. Johnson, C. C. Richardson, *Proc. Natl. Acad. Sci. U.S.A.* **101**, 4373 (2004).
- D. L. Kaplan, *J. Mol. Biol.* **301**, 285 (2000).
- J. Thirlway *et al.*, *Nucleic Acids Res.* **32**, 2977 (2004).
- L. Stordal, R. Maurer, *J. Bacteriol.* **178**, 4620 (1996).
- P. Chang, K. J. Marians, *J. Biol. Chem.* **275**, 26187 (2000).
- Y. B. Lu, P. V. A. L. Ratnakar, B. K. Mohanty, D. Bastia, *Proc. Natl. Acad. Sci. U.S.A.* **93**, 12902 (1996).
- R. Maurer, A. Wong, *J. Bacteriol.* **170**, 3682 (1988).
- C. A. Wu, E. L. Zechner, K. J. Marians, *J. Biol. Chem.* **267**, 4030 (1992).
- R. Galletto, M. J. Jezewska, W. Bujalowski, *J. Mol. Biol.* **343**, 83 (2004).
- M. J. Jezewska, S. Rajendran, W. Bujalowski, *J. Biol. Chem.* **273**, 9058 (1998).
- J. E. Corn, P. J. Pease, G. L. Hura, J. M. Berger, *Mol. Cell* **20**, 391 (2005).
- S. J. Lee, C. C. Richardson, *Proc. Natl. Acad. Sci. U.S.A.* **99**, 12703 (2002).
- This research was supported by NIH grant GM57510 to T.A.S. We thank P. Soutlanas for the expression plasmids. Coordinates and structure factors of crystal forms BH1, BH2, B1, and B2 have been deposited under accession codes 2R6A, 2R6C, 2R6D, and 2R6E, respectively.

Supporting Online Material

www.sciencemag.org/cgi/content/full/318/5849/459/DC1

Materials and Methods

SOM Text

Figs. S1 to S7

Tables S1 and S2

References

3 July 2007; accepted 11 September 2007

10.1126/science.1147353

Network Analysis of Oncogenic Ras Activation in Cancer

Edward C. Stites,^{1,2,3} Paul C. Trampont,¹ Zhong Ma,¹ Kodi S. Ravichandran^{1*}

To investigate the unregulated Ras activation associated with cancer, we developed and validated a mathematical model of Ras signaling. The model-based predictions and associated experiments help explain why only one of two classes of activating Ras point mutations with in vitro transformation potential is commonly found in cancers. Model-based analysis of these mutants uncovered a systems-level process that contributes to total Ras activation in cells. This predicted behavior was supported by experimental observations. We also used the model to identify a strategy in which a drug could cause stronger inhibition on the cancerous Ras network than on the wild-type network. This system-level analysis of the oncogenic Ras network provides new insights and potential therapeutic strategies.

Ras is a small guanosine triphosphatase (GTPase) that binds the guanine nucleotides guanosine triphosphate (GTP)

and guanosine diphosphate (GDP) (1, 2). Ras bound to GTP (Ras_{GTP}) is the "active" form with which downstream effector proteins spe-

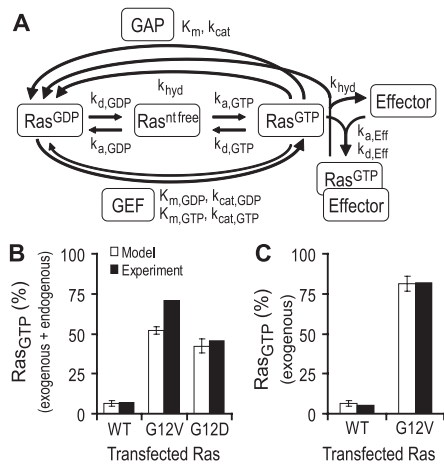


Fig. 1. The Ras GTPase signaling module and model validation. **(A)** We define the Ras GTPase signaling module to include Ras and the proteins with which it directly interacts (GEFs, GAPs, and Effectors). The model included all reactions of Ras with these proteins, as well as the reactions intrinsic to Ras (nt free refers to nucleotide-free). **(B)** Predicted steady-state percentage of GTP-bound total Ras in Ras^{WT/WT} cells transfected with Ras^{WT}, Ras^{G12V}, or Ras^{G12D}. **(C)** Predicted steady-state percentage of exogenous Ras bound to GTP in Ras^{WT/WT} cells transfected with Ras^{WT} or Ras^{G12V}. **(B** and **C)** Experimental data were from published studies (12–14). Model predictions are mean ± SD for nine different sets of protein concentration parameters.

cifically interact, thus propagating intracellular signals (1, 2). Several downstream effector pathways are associated with cancer (3). Activating point mutations in the three isoforms of Ras are frequently found in human cancers (4). Although less than 5% of Ras is typically bound to GTP under basal resting conditions, over 50% of Ras is bound to GTP in cells with an activating Ras point mutation under the same conditions. High levels of unregulated Ras activation are thought to have a causal role in the development of cancer (1).

The activation state of Ras reflects a complex balance of several processes that coordinately regulate Ras_{GTP} (Fig. 1A) (5). Guanine nucleotide exchange factors (GEFs) facilitate dissociation and exchange of bound nucleotide from Ras. Ras inactivation (by hydrolysis of bound GTP to GDP) can be done at a slow rate by Ras itself through its intrinsic GTPase activity. GTPase-activating proteins (GAPs) increase the rate of GTP hydrolysis. Associ-

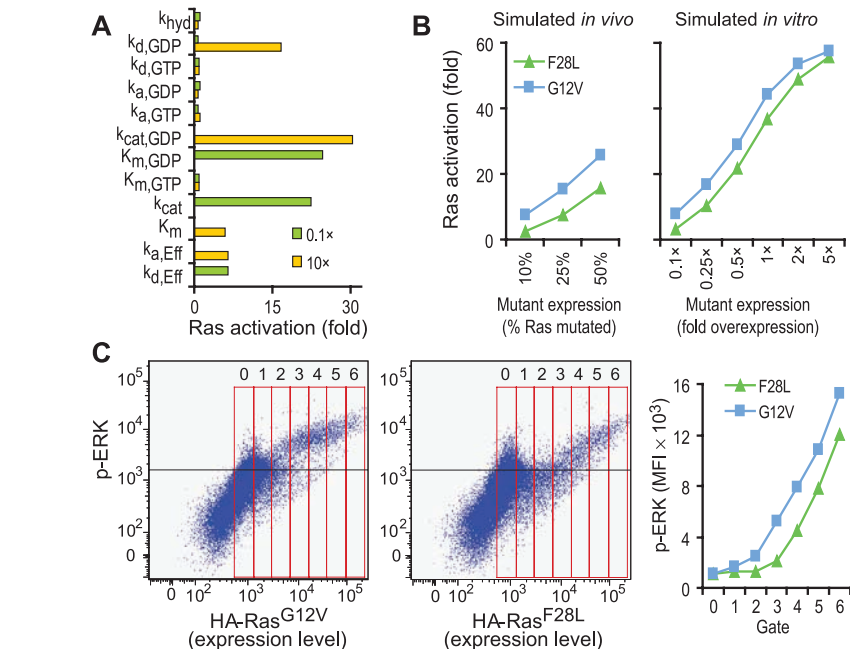


Fig. 2. A subset of Ras module properties can increase Ras signaling when altered. **(A)** Sensitivity analysis. The increase in Ras activation (total Ras-effector complex) due to an order of magnitude increase or decrease in each parameter of the Ras module. **(B)** Simulated *in vivo* and *in vitro* increases in Ras activation for fast-cycling (F28L) or GAP-insensitive (G12V) mutants. **(C)** (Left) Flow cytometry–based single-cell, quantitative assessment of Ras pathway activation (measured as phospho-ERK) as a function of expression levels of Ras^{F28L} or Ras^{G12V} in HEK-293T cells (50,000 events plotted for each). HA, hemagglutinin tagged. (Right) Plotting of the mean fluorescent intensity (MFI) for pERK versus mutant Ras protein expression levels, using the gates specified. These data are representative of two independent experiments. See fig. S1 for additional data under different transfection conditions.

ation of Ras_{GTP} with effector proteins can prevent regulatory enzymes from acting on Ras_{GTP} and can also prevent nucleotide dissociation, thus resulting in a sequestration of Ras_{GTP} (6). Attempts to understand Ras activation in a systems-level, cellular context must also consider concentrations of proteins that regulate Ras and the rate constants for their reactions.

We developed a mathematical model of the Ras signaling module using established methods for describing signal transduction networks (7), including heterotrimeric GTP-binding protein (G protein) and small GTPase signaling networks (8, 9). The model accounts for GEF-catalyzed exchange, GAP-catalyzed hydrolysis, intrinsic association and dissociation of nucleotide from Ras, hydrolysis of GTP by Ras, and interaction of Ras_{GTP} with downstream effectors (10) (Fig. 1A). All rate constants needed to characterize these reactions have been measured previously for wild-type Ras (Ras^{WT}) (table S1). The magnitude of change has been measured for properties that differ largely from those of Ras^{WT} for several Ras mutants (table S2). The model requires 20 parameters to describe a module with Ras^{WT}. When both wild-type and mutant Ras are present, 14 additional parameters are

required to incorporate the biochemical differences between them. Multiple sets of protein concentrations were considered to assess the robustness of our model because different cell types could express varying concentrations of module proteins [supporting online material (SOM) text]. Because oncogenic Ras point mutants result in increased steady-state concentrations of cellular Ras_{GTP} in the absence of stimulation, we focused on the steady-state behavior of Ras. We calculate two measures of Ras signaling output: the percentage of total Ras bound to GTP, and the concentration of Ras-effector complex formed (referred to here as “Ras activation”). When we discuss Ras activity, we refer to Ras signaling activity and not Ras GTPase activity. To test our model, we modeled a Ras^{WT} cell transfected with Ras^{WT}, Ras^{G12V}, or Ras^{G12D} [which indicate point mutations in which, for example, Gly¹² is replaced by Val (G12V) (11)] to predict the percentage of total Ras (endogenous and exogenous), or exogenous Ras bound to GTP. Predictions were robust and matched well with experimental data (12–14) (Fig. 1, B and C, and table S3). Model predictions for the Ras GAP-deficient state associated with neurofibromatosis also support the ability of the model to make robust, quantitative predictions (SOM text).

¹Bernie B. Carter Center for Immunology Research and the Department of Microbiology, University of Virginia, Charlottesville, VA 22908, USA. ²Medical Scientist Training Program, University of Virginia, Charlottesville, VA 22908, USA. ³Interdisciplinary Program of Biophysics, University of Virginia, Charlottesville, VA 22908, USA.

*To whom correspondence should be addressed. E-mail: Ravi@virginia.edu

Presumably, a mutation that disrupts any of the processes that regulate Ras could result in pathological Ras activation. However, only a few modes of deregulation are actually found in disease. We used our model to investigate the sensitivity of Ras activation to changes in each module property and found that Ras activation was largely affected by only four properties (Fig. 2A). There was good correlation between these four properties and the known physiological and pathological mechanisms of Ras pathway activation in many cancers (SOM text) (2). This analysis may help explain why only a limited number of the network properties result in pathological Ras activation when altered, i.e., network behavior is such that a disruption in a module property typically has a minimal effect on Ras activation.

Two of the properties that the model predicts will strongly influence Ras activation are altered in Ras point mutants with in vitro trans-

formation potential: the rate of GDP dissociation from Ras ($k_{\text{diss,GDP}}$) is increased for fast-cycling mutants (e.g., Ras^{F28L}), and the k_{cat} for the GAP reaction is strongly decreased for GAP-insensitive mutants (e.g., Ras^{G12V}). Although both GAP-insensitive and fast-cycling Ras mutants have in vitro transformation potential (15, 16), only GAP-insensitive Ras mutants are commonly found in cancers (2). When modeled at concentrations consistent with a spontaneous mutation in vivo, fast-cycling Ras^{F28L} showed approximately half the increase in forming Ras-effector complex of GAP-insensitive Ras^{G12V} (Fig. 2B). However, when we simulated concentrations consistent with the conditions of in vitro transformation assays, the difference between fast-cycling and GAP-insensitive mutants was reduced, and higher activation levels were achieved for both mutant classes (Fig. 2B). Results were similar for alternative sets of module protein concentrations (fig. S1).

To test these predictions experimentally, we used flow cytometry to obtain quantitative, single-cell measurements of active Ras as a function of mutant expression level for either GAP-insensitive Ras^{G12V} or fast-cycling Ras^{F28L}. The amount of activated, phosphorylated extracellular signal-regulated kinase (pERK) was used as a readout of Ras activation (2). Expression of small amounts of Ras^{F28L} caused production of less pERK than did similar amounts of Ras^{G12V} (Fig. 2C and fig. S2), in agreement with our model (Fig. 2B). Both mutants caused large amounts of pERK at higher expression levels (Fig. 2C). Thus, our computational and experimental results suggest that fast-cycling Ras point mutants may not be found in cancers because they cause a smaller increase in Ras signal amplitude than GAP-insensitive mutants for the concentration range likely to occur with spontaneous mutations.

Biochemical measurements have identified three differences between Ras^{WT} and Ras^{G12V} that might contribute to increased Ras_{GTP}: (i) The rate of GTP hydrolysis for Ras^{G12V} seems unaffected by the addition of GAP (GAP insensitivity) (17); (ii) the intrinsic GTPase activity of Ras^{G12V} is approximately one order of magnitude slower than that of Ras^{WT} (reduced intrinsic GTPase activity) (18); and (iii) the affinity of Ras^{G12V} for its downstream effector Raf is approximately doubled (increased effector affinity) (19). GAP insensitivity has been proposed as the primary cause of increased Ras activation (1). However, this hypothesis has not been testable experimentally because Ras^{G12V} exhibits all of these altered biochemical properties simultaneously.

In our model, GAP insensitivity alone increased the percentage of total Ras existing as Ras_{GTP} to about half that predicted when all mutant properties were included (Fig. 3A and table S4). In contrast, reduced intrinsic GTPase activity and increased effector affinity individually had minimal predicted effect on Ras activation (Fig. 3A; table S4). Reduced intrinsic GTPase activity did cause a predicted further increase when combined with GAP insensitivity, and increased effector affinity also caused a small increase when combined with GAP insensitivity (Fig. 3A). Essentially similar results were obtained when parameters for Ras^{G12D} were used, which suggests that these results are applicable to other GAP-insensitive Ras point mutants (table S5).

The combination of GAP insensitivity, reduced GTPase activity, and increased effector affinity did not account for all of the increased Ras activation. Although Ras^{G12V} is GAP-insensitive, it associates with GAP proteins (20), and could competitively inhibit Ras GAP activity on Ras^{WT}. In our model, formation of Ras_{GTP} was increased when competitive inhi-

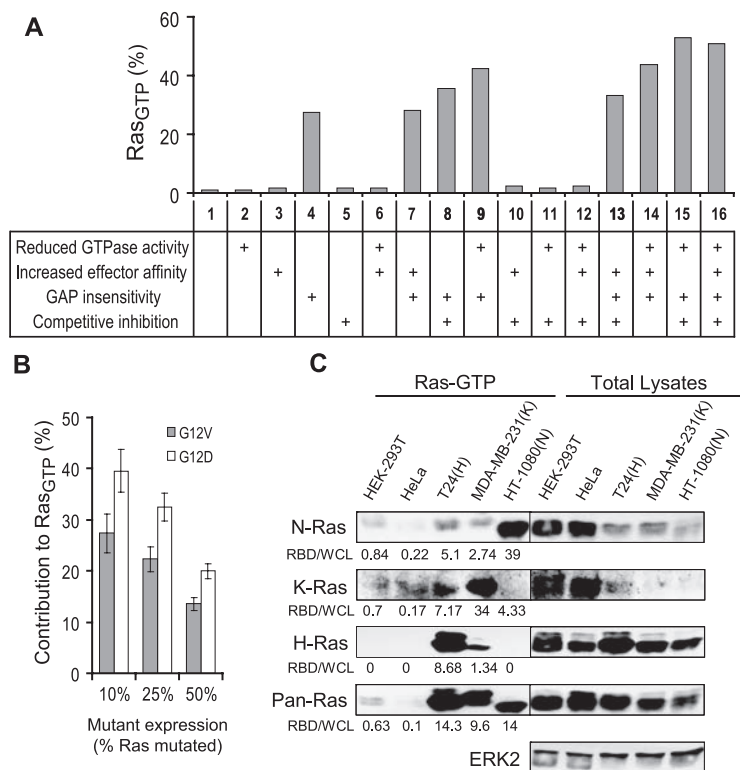


Fig. 3. Effects on Ras activation due to the multiple biochemical changes of the Ras^{G12V} point mutant. (A) Predicted percentage of GTP-bound total Ras for a Ras^{G12V/WT} module when the altered biochemical properties of the Ras^{G12V} mutant are considered as individual entities or in combination. (B) Relative contribution of competitive inhibition of Ras GAPs by Ras^{G12V} or Ras^{G12D} to the total increase in Ras_{GTP} formed for different percentages of total Ras mutated. Results presented are means \pm SD for the nine different sets of protein concentrations. (C) Proportion of total Ras as Ras_{GTP} in cell lines with GAP-insensitive Ras mutants (T24, MDA-MB-231, and HT1080) and in cell lines without a known Ras mutation (HEK-293T and HeLa), measured by precipitation of lysates using the Ras_{GTP}-binding domain of Raf (RBD). To determine the fraction of a given isoform bound to GTP, immunoblotting was done using isoform-specific antibodies or a pan-Ras antibody. The signals for Ras_{GTP} in the different cell lines were normalized against total cellular Ras in the same cell line. Results reflect two to five independent experiments, and the differences were significant ($P < 0.05$, Student's t test).

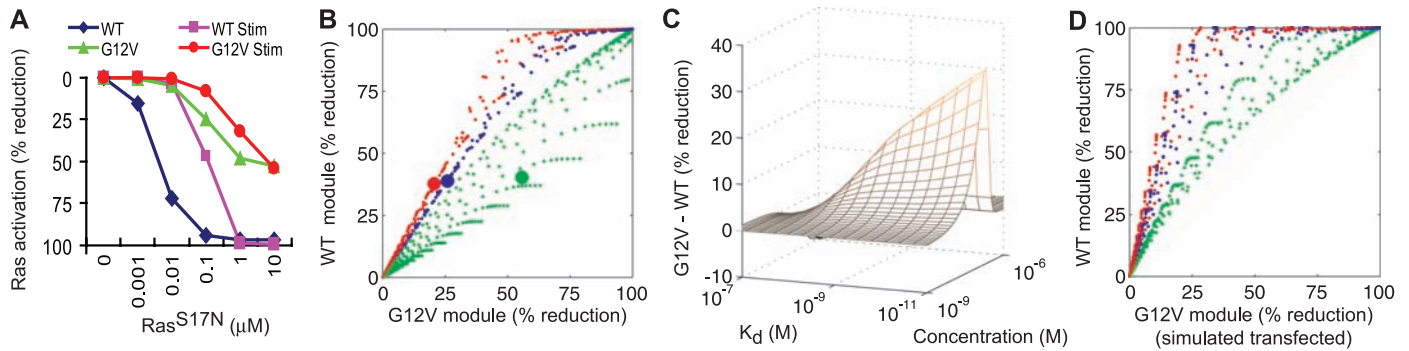


Fig. 4. Model-based analysis of pharmacological strategies to preferentially inhibit the cancerous Ras module. **(A)** Dose-dependent decrease in Ras activation (concentration of Ras-effector complex) caused by dominant-negative Ras^{S17N} for wild-type Ras networks expressing exogenous Ras^{WT} or Ras^{G12V} and in the presence or absence of stimulation. **(B)** Predicted reduction in Ras activation for the different drug strategies on the Ras^{G12V/WT} module and on the stimulated Ras^{WT/WT} module. Each point corresponds to one of 600 total conditions (15 different affinities and 40

different concentrations) for each of the three strategies. Drug A, red; drug B, green; drug C, blue. Large filled circles represent effects for relevant drug-Ras interactions at $K_d = 1$ nM and drug concentration at 0.15 μ M. **(C)** The difference in percent reduction between oncogenic G12V module inhibition and wild-type module inhibition for drug B, presented as a function of drug affinity and concentration. **(D)** Same as **(B)**, but the G12V module is now modeled as a Ras^{WT/WT} cell transfected with exogenous Ras^{G12V}.

dition of Ras GAP was combined with GAP insensitivity (Fig. 3A). This increase did not result from changes in the fraction of Ras^{G12V} that was GTP-bound (~85% in both cases), rather it was due to an increase in the GTP-bound fraction of Ras^{WT} (from 1 to 15%) (table S4). Results were similar when alternative sets of module protein concentrations were modeled (fig. S3). This analysis has been done with the assumption that 50% of total cellular Ras is mutated. As there are three isoforms, we performed the same analysis for cases when less than 50% of total cellular Ras is mutated and obtained similar results (tables S6, S7). The relative contribution of competitive inhibition on Ras activation increased when mutated Ras made up a smaller fraction of total Ras in the cell (Fig. 3B). This further suggests competitive inhibition is likely to occur after point mutation in one of the *ras* genes in the cell.

To test the predicted effect of competitive inhibition of Ras GAPs on Ras activation we performed a Ras-binding domain (RBD) pull-down assay on three cancer cell lines that harbor GAP-insensitive Ras mutations (T24: H-Ras^{G12V}; HT1080: N-Ras^{Q61L}; MDA-MB-231: K-Ras^{G13D}) and, as controls, two cell lines in which activating Ras mutations have not been described (HeLa, HEK-293T). We found a statistically significant increase in the proportion of GTP-bound Ras^{WT} for the cells harboring GAP-insensitive Ras point mutants (Fig. 3C). Taken together, our combined computational and experimental work uncovered a systems-level process that our simulations predict could contribute upwards of 30% of the Ras_{GTP} found in a cell with an activating point mutation. Our results indicate that cancers will likely display significant heterogeneity because of secondary activation of other WT Ras isoforms in the same cell.

Ideally, a therapeutic strategy to inhibit Ras signaling would have a much stronger effect on diseased cells with an oncogenic Ras mutation than on healthy cells without a Ras mutation (2). The Ras signaling network is characterized by different properties for cancerous and non-cancerous cells, and a nonlinear dynamical system can have quantitatively and/or qualitatively different behaviors for different sets of system parameters. We therefore hypothesized that a drug binding both Ras^{G12V} and Ras^{WT} with equal affinity could block Ras signaling in the cancerous network more than the wild-type network. To first test the ability of our model to assess possible pharmaceutical strategies, we compared the dose-dependent inhibition of Ras activation by dominant-negative Ras on a network expressing exogenous Ras^{G12V} or Ras^{WT}. The model showed that dominant-negative Ras^{S17N} had a stronger effect on the wild-type network (Fig. 4A and fig. S4). This is consistent with experimental observations that Ras^{S17N} inhibited Ras^{WT} signaling more than it did oncogenic Ras signaling (21). This observation, once considered “unexpected” (21), is readily explained from our systems-level model.

To search for a therapeutically beneficial strategy, we extended our model to examine three possible strategies of drug intervention: (i) a hypothetical drug A that binds and sequesters Ras_{GDP}, (ii) a potential drug B that binds and sequesters Ras_{GTP}, and (iii) a drug C that binds and sequesters both Ras_{GDP} and Ras_{GTP} equally well (fig. S5). We ran simulations of the extended model to test each drug strategy. Only drug B caused a greater reduction in Ras-effector interactions in the cancerous network (Ras^{G12V/WT}) than in the wild-type network (Ras^{WT/WT}). In contrast, drug A and drug C caused a greater reduction in Ras-effector interactions for the Ras^{WT/WT} signaling module than for the

Ras^{G12V/WT} module (Fig. 4B). Drug B was predicted to have this behavior for a wide range of conditions (Fig. 4C). Results were similar when alternative sets of module protein concentrations were modeled (fig. S6). Previous experimental studies of potential Ras inhibitors have used Ras^{WT/WT} cells that had been transfected with Ras^{G12V} (22, 23). In our simulations, drug B was no longer selective under these conditions (Fig. 4D). Thus, the use of Ras^{G12V}-transfected cell lines may yield false-negatives when used to screen for drugs that selectively target cancerous cells.

Oncogenic Ras has been well studied at the genetic, biochemical, and whole-animal levels. This molecular network level analysis of the Ras signaling module provided a bridge between the biochemical data at the protein level and Ras activation at the cellular level. The systems-level analysis of the wild-type Ras network and an oncogenic Ras network also identified a strategy that selectively targeted the mutant network as a result of quantitative differences between the two networks. Similar strategies might be found for other networks where mutations alter biochemical properties and result in pathological deregulation. These results highlight the promise of systems-level mathematical models to study signaling pathways altered in disease and to identify potential drug strategies.

References and Notes

1. M. Malumbres, M. Barbacid, *Nat. Rev. Cancer* **3**, 459 (2003).
2. J. Downward, *Nat. Rev. Cancer* **3**, 11 (2003).
3. G. A. Repasky, E. J. Chenette, C. J. Der, *Trends Cell Biol.* **14**, 639 (2004).
4. J. L. Bos, *Cancer Res.* **49**, 4682 (1989).
5. M. S. Boguski, F. McCormick, *Nature* **366**, 643 (1993).
6. C. Herrmann, G. Horn, M. Spaargaren, A. Wittinghofer, *J. Biol. Chem.* **271**, 6794 (1996).

7. B. B. Aldridge, J. M. Burke, D. A. Lauffenburger, P. K. Sorger, *Nat. Cell Biol.* **8**, 1195 (2006).
8. N. I. Markevich *et al.*, *Syst. Biol. (Stevenage)* **1**, 104 (2004).
9. S. J. Bornheimer, M. R. Maurya, M. G. Farquhar, S. Subramaniam, *Proc. Natl. Acad. Sci. U.S.A.* **101**, 15899 (2004).
10. Materials and methods are available as supporting material on Science Online.
11. Single-letter abbreviations for the amino acid residues are as follows: A, Ala; C, Cys; D, Asp; E, Glu; F, Phe; G, Gly; H, His; I, Ile; K, Lys; L, Leu; M, Met; N, Asn; P, Pro; Q, Gln; R, Arg; S, Ser; T, Thr; V, Val; W, Trp; and Y, Tyr.
12. G. Bollag *et al.*, *J. Biol. Chem.* **271**, 32491 (1996).
13. J. B. Gibbs, M. S. Marshall, E. M. Scolnick, R. A. Dixon, U. S. Vogel, *J. Biol. Chem.* **265**, 20437 (1990).
14. S. Boykevich *et al.*, *Curr. Biol.* **16**, 2173 (2006).
15. L. A. Feig, G. M. Cooper, *Mol. Cell. Biol.* **8**, 2472 (1988).
16. G. Patel, M. J. MacDonald, R. Khosravi-Far, M. M. Hisaka, C. J. Der, *Oncogene* **7**, 283 (1992).
17. M. R. Ahmadian, U. Hoffmann, R. S. Goody, A. Wittinghofer, *Biochemistry* **36**, 4535 (1997).
18. J. F. Eccleston, K. J. Moore, G. G. Brownbridge, M. R. Webb, P. N. Lowe, *Biochem. Soc. Trans.* **19**, 432 (1991).
19. E. Chuang *et al.*, *Mol. Cell. Biol.* **14**, 5318 (1994).
20. U. S. Vogel *et al.*, *Nature* **335**, 90 (1988).
21. D. W. Stacey, L. A. Feig, J. B. Gibbs, *Mol. Cell. Biol.* **11**, 4053 (1991).
22. N. E. Kohl *et al.*, *Science* **260**, 1934 (1993).
23. G. L. James *et al.*, *Science* **260**, 1937 (1993).
24. We are grateful to S. Walk for the HA-Ras plasmids, and the members of the Ravichandran lab for helpful

discussions. E.S. was supported through a cancer training grant (NCI), and Z.M. was supported by a Biodefense training grant (NIAID). This work was supported in part by a grant from the NIGMS (to K.S.R.).

Supporting Online Material

www.sciencemag.org/cgi/content/full/318/5849/463/DC1
Materials and Methods
SOM text
Figs. S1 to S7
Tables S1 to S7
References

4 May 2007; accepted 6 September 2007
10.1126/science.1144642

Light-Responsive Cryptochromes from a Simple Multicellular Animal, the Coral *Acropora millepora*

O. Levy,¹ L. Appelbaum,² W. Leggat,¹ Y. Gothlif,³ D. C. Hayward,^{4,6}
D. J. Miller,^{5,6} O. Hoegh-Guldberg^{1,5}

Hundreds of species of reef-building corals spawn synchronously over a few nights each year, and moonlight regulates this spawning event. However, the molecular elements underpinning the detection of moonlight remain unknown. Here we report the presence of an ancient family of blue-light–sensing photoreceptors, cryptochromes, in the reef-building coral *Acropora millepora*. In addition to being cryptochrome genes from one of the earliest-diverging eumetazoan phyla, *cry1* and *cry2* were expressed preferentially in light. Consistent with potential roles in the synchronization of fundamentally important behaviors such as mass spawning, *cry2* expression increased on full moon nights versus new moon nights. Our results demonstrate phylogenetically broad roles of these ancient circadian clock–related molecules in the animal kingdom.

Many organisms possess endogenous clocks that respond to rhythmic changes in light and temperature caused by Earth's rotation (1, 2), allowing them to anticipate daily and annual environmental cycles and to adjust their biochemical, physiological, and behavioral processes accordingly (1). The circadian clock uses cues such as light to entrain endogenous oscillators, which in turn control rhythmic outputs of a wide range of organisms (2). Even simple animals such as medusae (scyphozoan or hydrozoan cnidarians) have specialized light-

sensing organs known as ocelli (eyes) or eyespots. These photoreceptors react to changes in light intensity and are responsible for phototaxis and other behavioral responses to light (3). However, anthozoan cnidarians (corals, sea anemones, and sea pens) lack specialized sense organs yet display photosensitive behavior (4–11). The synchronized mass spawning on the Great Barrier Reef (GBR) in Australia is a spectacular example of the photosensitive responses exhibited by these organisms (7–9). Over several nights after the full moon in late spring each year, hundreds of coral species spawn en masse, with the final trigger being changes in the lunar irradiance intensity (8, 11).

The specific cellular mechanisms involved in light detection by reef-building corals (Anthozoa, Cnidaria) have remained elusive. Biophysical data (4) show that corals are highly sensitive to blue light, which is also known to entrain the circadian clocks of insects and mammals (12) via cryptochromes (CRYs), which are DNA photolyase–like photoreceptor proteins. The roles of crypto-

chromes differ subtly between mammals and insects; the proteins function as circadian oscillator components in *Mus* but as photoreceptors for clock entrainment in *Drosophila* (13, 14). To date, CRYs have been identified only in higher animals such as vertebrates and insects, although related (and divergent) proteins have been reported in plants and eubacteria (12).

We used degenerate primers based on sequences conserved between *Mus*, *Drosophila*, *Xenopus*, and *Danio* to clone two *cry* genes from the coral *Acropora millepora* (15). The proteins encoded by the genes *cry1* and *cry2* each contain an N-terminal photolyase-related region (PHR) bearing two chromophore-binding domains and C-terminal domains extending 54 (CRY1) or 27 (CRY2) amino acids in length. *cry1* and *cry2* were also identified in expressed sequence tag (EST) data sets generated from *A. millepora* larvae (16), as were two additional genes known here as *cry3* (15) and *cry-dash*. Because the cDNA library was constructed from aposymbiotic larvae, these *cry* genes are likely to be from coral rather than from associated symbiotic algae or marine microbes.

Phylogenetic analyses (Fig. 1) emphasize the similarity of coral CRYs and their vertebrate counterparts. Coral CRY1 belongs to the mammalian-type (m-type) CRY group. Both CRY1 and CRY2 are only distantly related to the *Drosophila*-type CRYs. CRY2 more closely resembles the *Danio* photoreceptor candidate CRY4-type (17) and is basal to the clade comprising both the m-type CRYs and the (6–4) photolyases. Coral CRY-DASH is a typical CRY-DASH protein (18) and is basal in the animal CRY-DASH clade. This analysis suggests that coral CRYs may represent ancestral members of the protein family in the animal kingdom, potentially providing insights into the origins of light perception in animals.

On the GBR, we investigated (15) whether the expression of *cry1* and *cry2* in corals is rhythmic only under light/dark (LD) cycles as in *Drosophila* (13) or driven by an endogenous

¹Centre for Marine Studies, University of Queensland, St. Lucia 4072 QLD, Australia. ²Center for Narcolepsy and Howard Hughes Medical Institute, Stanford University, Palo Alto, CA, USA. ³Department of Neurobiochemistry, Faculty of Life Sciences, Tel Aviv University, Israel. ⁴Research School of Biological Sciences, Australian National University, Canberra ACT 2601, Australia. ⁵Australian Research Council (ARC) Centre of Excellence for Coral Reef Studies, James Cook University, Townsville, QLD 4811, and University of Queensland, St. Lucia 4072 QLD, Australia. ⁶ARC Centre for the Molecular Genetics of Development, Research School of Biological Sciences, Australian National University, Canberra, ACT 2601, Australia.